Journal of Microscopy

Journal of Microscopy, Vol. 242, Pt 2 2011, pp. 216–220
Received 27 August 2010; accepted 24 October 2010

doi: 10.1111/j.1365-2818.2010.03472.x

Quantitative measurements of magnetic stray field dynamics of Permalloy particles in a photoemission electron microscopy

S.A. NEPIJKO*,†, A. KRASYUK‡, A. OELSNER§, C.M. SCHNEIDER# & G. SCHÖNHENSE*

**Institute of Physics, University of Mainz, Mainz, Germany*

†Institute of Physics, National Academy of Sciences of Ukraine, Kiev, C.I.S./Ukraine

‡Max Planck Institute of Microstructure Physics, Halle/Saale, Germany

§Surface Concept GmbH, Mainz, Germany

#Institute of Solid State Research IFF-6, Electronic Properties, Research Centre Jülich, Jülich, Germany

Key words. Magnetic stray fields, magnetization reversal, Permalloy particle, photoemission electron microscope.

Summary

By example of a Permalloy particle (40×40 μm^2 size, 30 nm thickness) we demonstrate a procedure to quantitatively investigate the dynamics of magnetic stray fields during ultrafast magnetization reversal. The measurements have been performed in a time-resolving photoemission electron microscope using the X-ray magnetic circular dichroism. In the particle under investigation, we have observed a flux-closure-dominated magnetic ground structure, minimizing the magnetic stray field outside the sample. A fast magnetic field pulse introduced changes in the micromagnetic structure accompanied with an incomplete flux closure. As a result, stray fields arise along the edges of domains, which cause a change of contrast and an image deformation of the particles geometry (curvature of its edge). The magnetic stray fields are calculated from a deformation of the X-ray magnetic circular dichroism (XMCD) images taken after the magnetic field pulse in a 1 ns interval. These measurements reveal a decrease of magnetic stray fields with time. An estimate of the lower limit of the domain wall velocity yields about 2×10^3 m s^{-1}.

Introduction

The magnetization reversal of ferromagnetic particles and subsequent changes in the shape of magnetic domains also result in changes in the magnetic stray fields emanating from these domains. Such stray fields arise, for example, at domain boundaries and of the magnetic elements edges as a result of incomplete closing of magnetic flux inside the particle. In electron beam-based microscopies such as scanning electron or emission electron microscopy, these external fields cause a deflection of the electrons escaping from the object surface. In the images they produce a deformation of the edges of the domains and particle edges observed. Quantitative relations between the value of the induction of the local magnetic fields on the object surface and the value of the shift of the image details at the microscope screen were considered in detail by Dyukov *et al.* (1991) and Nepijko *et al.* (2000, 2002a). The measurement procedures of static magnetic fields with the use of emission electron microscopy (PEEM) have been described by Krasyuk *et al.* (2007) and Nepijko *et al.* (2002a, 2003).

Similarly, by means of the method of time-resolved PEEM, quantitative measurements of *dynamic* magnetic fields may be realized. For this purpose, these investigations must be based on a time-dependent sequence of PEEM images. In the simplest case, the distance in time between these images may be chosen as $\Delta t = \text{const}$. If one calculates the local magnetic fields of the object under investigation for each individual PEEM image, then one can trace the alteration of these field distributions in time.

The first dynamic investigations of the domain structure of ferromagnetic particles with the help of photoemisson electron microscopy in combination with synchrotron light excitation are described by Choe *et al.* (2004), Krasyuk *et al.* (2003), Oelsner *et al.* (2004) and Vogel *et al.* (2003). This technique allows one to visualize magnetic domains using the XMCD (Schneider & Schönhense, 2002; Stöhr *et al.*, 1993). The intensity of secondary photoelectrons during the excitation at an absorption edge of a particular magnetic material by circularly polarized photons is determined by the mutual

Correspondence to: S. A. Nepijko, Institute of Physics, University of Mainz, Staudingerweg 7, 55099 Mainz, Germany. Tel: +49 6131 3925412; fax: +49 6131 3923807; e-mail: nepijko@uni-mainz.de

orientation between the magnetization vector within the magnetic domains and the propagation direction of the X-rays. The intensity is maximal (minimal) if their directions coincide (are opposite). The magnetic regions with other orientations are distinguished as areas of different grey levels in the PEEM image. This magnetic imaging approach provides an inherent element specificity.

The present paper demonstrates the quantitative investigation of magnetic stray field dynamics during magnetization reversal with the help of time-resolved PEEM for the example of a Permalloy particle with a few tens of micrometres in size and a few tens of nanometres in thickness.

Experimental

The specimens used for our investigations consisted of a microstructured thin film system. We started out with a SiO_x/Si substrate, onto which copper microstrip lines 50 μm in width and 200 nm in thickness were photolithographically prepared in a first step. Onto these lines, we deposited a 30 nm Permalloy film covered by 2 nm of copper. This film was again microstructured in small elements by photolithography and ion milling. In this way square Permalloy particles of 40×40 μm^2 were accurately placed onto the microstrip lines. Before carrying out PEEM investigations, the specimens were subjected to a cleaning step by mild ion bombardment in the photoemission microscope. This procedure decreased the thickness of the protective copper layer to approximately 1 nm.

The geometry of the coplanar wave guide taking into account the materials used was chosen so as to yield an impedance of 50 Ω, in order to match to the remaining electric circuit. In this case, we ensured a transmission of the remagnetizing current pulse through the microstrip lines with minimal losses. The current pulse was fed into the vacuum chamber by means of coaxial cables and connectors characterized by a high frequency bandwidth of about 10 GHz. The direction of the magnetic field in the microstrip line was reversed by exchanging the input and output lines.

The measurements of the magnetic field emanating from the Permalloy particles were carried out with the use of a stroboscopic imaging technique in the photoemission electron microscope. The photoelectrons were excited by circularly polarized soft X-ray photons exactly at the absorption edges of the respective magnetic material (Fe or Ni). The synchrotron radiation was supplied via the UE56/II-PGM beamline at BESSY II (Berlin). For time-resolved measurements, we used the single bunch mode of BESSY, delivering photon pulses with widths of less than 100 ps (in our measurements 45 ps) at a fixed repetition frequency of 1.25 MHz (repetition rate 800 ns). A precise cable delay served as time adjustment element between the bunch marker signal and the trigger input of the pulse generator. The generator produced a pulse of positive polarity with an amplitude of $U = 35$ V, duration of 8 ns and pulse rise time (leading edge) of approximately 300 ps. The magnetic field created by the current pulse on the surface of the microstrip line amounted to a few mT.

In the investigations described below, the spatial and temporal resolution had values of <100 nm and 125 ps, respectively. This measuring procedure is described in more detail by Oelsner *et al.* (2001, 2004).

Quantitative measurements of magnetic fields in dynamics

Fig. 1a illustrates the static XMCD-PEEM image of a Permalloy particle with dimensions 40×40 μm^2 and 30 nm in thickness, before it is affected by the current pulse creating the remagnetizing field. The boundaries of the magnetic domains

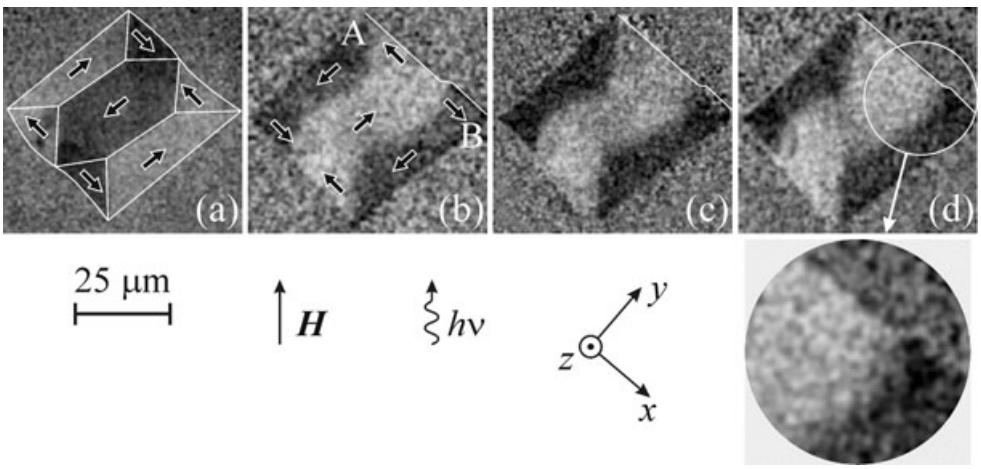

Fig. 1. XMCD-PEEM images of the Permalloy particle taken before (a) and at 0 (b), 1 (c) and 2 ns (d) after the magnetic field pulse. $\boldsymbol{H}$ and $h\nu$ denote the directions of remagnetization field and of illumination by circularly polarized synchrotron radiation (its projection on the sample surface); black arrows indicate the local magnetization direction. The photon energy was tuned to the Ni L_3 edge at $h\nu = 853$ eV. Insert shows a more detailed image of the area designated by a white circle in (d).

(their total number amounts to seven) are marked with white lines. The directions of the local domain magnetization are shown as black arrows. The wavy arrow hv depicts the direction of illumination by circularly polarized photons with energy of 853 eV (it was tuned to the Ni L_3 edge). After the effect of the current pulse, the particle's magnetization was reversed (Fig. 1b). The inversion of the domain contrast of all domains on the XMCD-PEEM image can be observed, that is the direction of magnetization of all the domains changed to opposite.

Fig. 1b corresponds to a certain time point after passage of the current pulse through the microstrip lines. We shall perform time reading t from this time point, that is Fig. 1b corresponds to $t = 0$. The magnetization reversal involves different micromagnetic processes on different time scales, such as magnetization rotation, domain nucleation and domain wall motion, which smear out the reversal event over a broader time interval, the slower processes leading to a 'relaxation' of the system. This is also seen from the comparison of the images of the particle in Fig. 1b, c and d, which have been acquired with time steps of $\Delta t = 1$ ns, that is in moments of time t equal to 0, 1 and 2 ns, respectively. Close inspection reveals that the image of the particle continues to deform with time: domain boundaries shift, the shape of the line AB changes, with which one of the edges of the particle is marked, and so on. The x-axis is directed along the AB edge. Deformation of the particle image decreases with increase of time t. It decreases in the sequence from Fig. 1b–d, but even in the last case, it remains sufficiently noticeable to measure bending of AB edge (see the insert). The insert shows more minutely the area in Fig. 1d designated by a white circle. Fig. 2a demonstrates the shifts of points along the edge AB of the particle. Here solid, dashed and dotted curves correspond to Fig 1b–d, respectively. For each of these curves one can calculate a magnetic field distribution created by the particle under investigation, and eo ipso trace the variation with time.

According to Eq. (4) in the work by Nepijko *et al.* (2002a) (see also Eq. (3) in the work by Nepijko *et al.* (2003)) the magnetic field along the x-axis on the object surface can be written as

$$B_{0x}(x) = -\frac{3}{4\pi}\sqrt{\frac{mE_0}{e}}\int_{-\infty}^{\infty}\frac{S_y(x-\xi) - S_y(x) + \xi S_y'(x)}{|\xi|^{5/2}}d\xi, \tag{1}$$

with $S_y(x)$ being the value of the observed shift in y-direction, E_0 the electrical field which accelerates the electrons over the object in the immersion objective of the electron microscope, e and m the charge and the mass of the electron, respectively. The object plane coincides with the Cartesian (x,y)-plane and the z-axis is perpendicular to it (as indicated in Fig. 1). As a result of the Lorentz force action, the deviation S_y is perpendicular to the tangential component of the magnetic field B_{0x}. As far as it concerns the component of magnetic field B_{0z}, normal to the object surface, it can be calculated with the help of the Hilbert transformation:

$$B_{0z}(x) = -\frac{1}{\pi}\int_{-\infty}^{\infty}\frac{B_{0x}(\xi)\,d\xi}{x-\xi}. \tag{2}$$

In practice, the mentioned integral transformations are easier to execute with the use of the Fourier transform. Let $F(f)$ be the Fourier transform of function $f(x)$. Then, transforming (1), we get

$$F(B_{0x}) = \sqrt{\frac{2mE_0}{\pi e}}F(S)\cdot\omega^{3/2}, \tag{3}$$

where ω is the spatial frequency, corresponding to the x coordinate. Thus, the task to calculate the distribution function of the magnetic field on the surface $B_{0x}(x)$ is solved as follows. The shift function $S_y(x)$ is measured at small equal intervals along the x-axis, using the image of the edge of the observed particle or magnetic domain. Then a fast Fourier transform (FTT) of this function is carried out. The resulting transformation is multiplied by the factors from Eq. (3); afterwards an inverse fast Fourier transform (IFFT) is made. As a result, we get the function $B_{0x}(x)$. The z-component

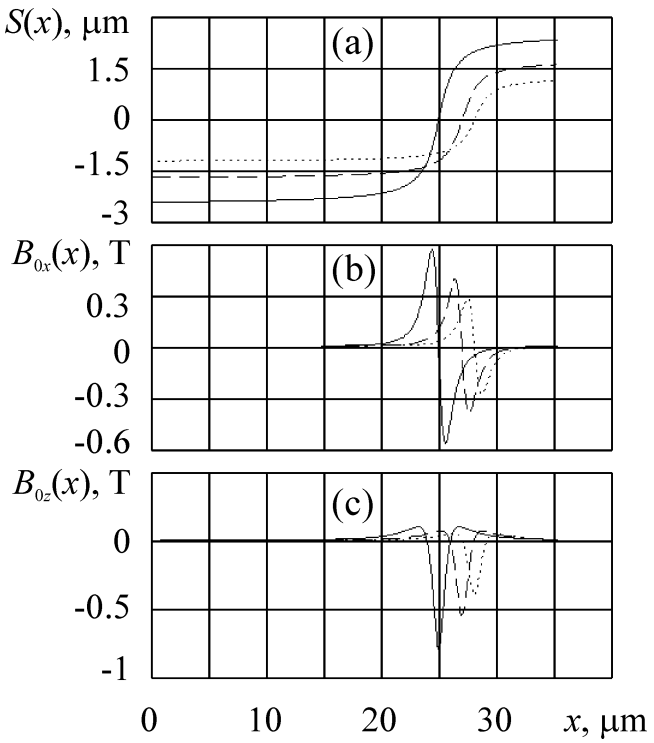

Fig. 2. Curves showing the shift $S(x)$ of the image points on the edge AB (see Fig. 1) of a Permalloy particle (a). Distributions of the transversal component of magnetic stray field $B_{0_x}(x)$ (b) calculated from (a) using expression (4) in the work by Nepijko *et al.* (2002a). The other component of magnetic stray fields $B_{0_z}(x)$ (c) was determined from (b) utilizing the condition that components of the magnetic field are linked with a Hilbert transform. These calculations were performed in the approximation of two-dimensional microfields. Solid, dashed and dotted lines correspond to the points at 0, 1 and 2 ns, respectively, after the magnetic field pulse.

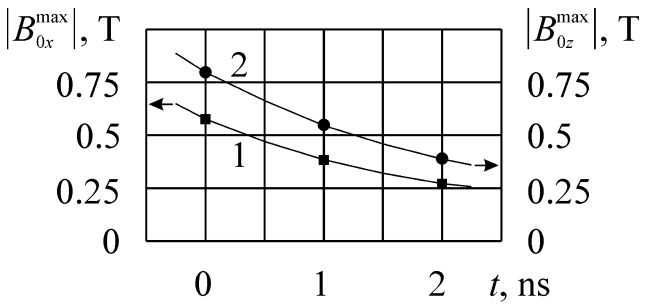

Fig. 3. Dynamics of the maximal value of tangential B_{0x}^{max} and normal B_{0z}^{max} components of the magnetic stray field.

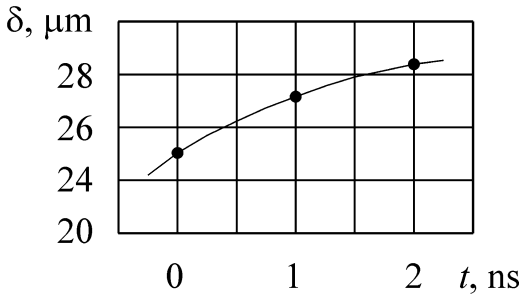

Fig. 4. Time dependence of the domain wall shift $\delta(t)$.

of the magnetic field $B_{0z}(x)$ is calculated by means of the Hilbert transformation, which is also easier with the use of Fourier transform.

The results of such calculations of the distribution of the tangential $B_{0x}(x)$ and the normal $B_{0z}(x)$ components of the magnetic stray field along the edge AB of the particle under investigation are given in Fig. 2b and c, respectively. Solid, dashed and dotted curves in Fig. 2b and c correspond to the moments of time $t = 0$, 1 and 2 ns.

The distribution of the normal component of the magnetic stray field along the edge AB of the particle is characterized by the absolute maximum value on the boundary between the domains (domain wall). On the left and right sides of it, spatial distributions of the tangential component of the magnetic stray field are identical, but are opposite in sign. Curves 1 and 2 in Fig. 3 were determined from Fig. 2b and c. They show the maximum value of the tangential and normal components of the magnetic stray field as a function of time, respectively. As one can see, the magnetic stray field weakens with time and asymptotically tends to zero because the relaxed state shows no image shift (Oelsner *et al.*, 2004). The displacement shift of this domain wall as a function of time is illustrated in Fig. 4. From the slope of the tangent to the curve of Fig. 4 we find a lower limit of the maximum domain wall velocity. It amounts to 2×10^3 m s^{-1}, which corresponds to the literature data (Raabe *et al.*, 2005; Krasyuk *et al.*, 2005, 2009). The velocity decreases with time after the magnetic field pulse.

The shift functions $S(x)$ in Fig. 2a are measured with accuracy not worse than 5%. It is determined by spatial resolution of PEEM studies performed by us. For XMCD-PEEM images in Fig. 1b–c, it amounts to a few tenths of micrometre, that is much worse than resolution limit of the used photoemission electron microscope. It is known that magnetic fields on the specimen impair the spatial resolution (Nepijko *et al.*, 2002b). At the same time, the dependences $B_{0x}(x)$ and $B_{0z}(x)$ in Fig. 2b and c calculated from experimental curves $S(x)$ in Fig. 2a are characterized by much lower accuracy. For tangential $B_{0x}(x)$ and normal $B_{0z}(x)$ components of magnetic field in Fig. 2b and c, the accuracy amounts to 10–15%. The accuracy of position of minima of the curves in Fig. 2c and position of crossing of the abscissa axis by the curves in Fig. 2b deteriorates as well and makes up ~0.5 μm. At the same time, the curves in Fig. 3 and 4 are derived from the curves in Fig. 2b and c. Hence the accuracy of determination of the maximal value of tangential $B_{0x}(x)$ and normal $B_{0z}(x)$ components of magnetic stray field in Fig. 3 amounts to 10–15%, and positions of points on the dependence $\delta(t)$ in Fig. 4 are characterized by an error up to 0.5 μm. The rate of motion of the domain wall determined from the slope of the curve $\delta(t)$ in Fig. 4 is $1.5 \div 2.5 \times 10^3$ m s^{-1}, that is, it is of the same order of magnitude 10^3 m s^{-1}.

The measurements show that the magnetization reversal takes place in two steps. In a first step, the magnetization in the domains reverses as a response to the magnetic field pulse on a time scale below 1 ns. This domain configuration, however, is still in an excited state, i.e. it does not yet correspond to the lowest energy state. It is characterized by a higher magnetic stray field contribution, which is reduced by a slower process of several ns involving domain wall motion. As a consequence, the stray field-free magnetic ground state of the system is obtained only after a relaxation on the ns time scale.

The technique described in the present paper is not restricted to a linescan along the edge of a particle. In order to map the stray fields in the whole field of view, reference points are deposited on the surface of the ferromagnetic object. That is realized with the deposition through a mask which can be a grid of dots of a paramagnetic material, for example silver. The dots will show up in contrast in the PEEM image. During the magnetization reversal, the distribution of the magnetic field on the surface of the object changes in time. Through the effect of these fields at every moment of time, the reference points of the grid in the PEEM image acquire characteristic shifts. According to these shifts and formulas shown in the present work, at every moment of time one determines the distribution of the magnetic field on the surface under investigation. Thus, time-resolved PEEM allows us to carry out quantitative measurements of the whole two-dimensional distribution of the magnetic field of the ferromagnetic object and its time dependence with <100 ps time resolution.

Conclusions

The magnetic stray field between the domains in a Permalloy particle with a size of 40 × 40 μm^2 and a thickness of 30 nm was quantitatively measured in dynamics (temporal resolution of 1 ns) immediately after a fast reversal of its magnetization. An attenuation of the stray field on a time scale of several ns has been observed. We have estimated the lower limit of the maximum velocity of the domain wall motion during the magnetization reversal. It amounts to 2×10^3 m s^{-1}.

The present method may be used in PEEM researches with excitation not only by high-energy synchrotron radiation, but also by low-energy radiation, which is produced, for example, by an UV lamp (Hg vapour source). It enables to investigate magnetic stray field dynamics and other properties of magnetic micro-objects with the help of photoemission electron microscope directly in the laboratory without utilization of synchrotron radiation sources.

References

Choe, S.-B., Acremann, Y., Scholl, A., Bauer, A., Doran, A., Stöhr, J. & Padmore, H.A. (2004). Vortex core-driven magnetization dynamics. *Science* **304**, 420–422.

Dyukov, V.G., Nepijko, S.A. & Sedov, N.N. (1991) *Electron Microscopy of Local Potentials*. Naukova Dumka, Kiev (in Russian).

Krasyuk, A., Nepijko, S.A., Oelsner, A., Schneider, C.M., Elmers, H.-J. & Schönhense, G. (2007) Magnetic stray fields of patterned Permalloy structures investigated by photoemission electron microscopy. *Appl. Phys.* A **88**, 793–796.

Krasyuk, A., Oelsner, A., Nepijko, S.A., Kuksov, A., Schneider, C.M. & Schönhense, G. (2003) Time-resolved photoemission electron microscopy of magnetic field and magnetisation changes. Appl. Phys. A **76**, 863–868.

Krasyuk, A., Wegelin, F., Nepijko, S.A., Elmers, H.J., Schönhense, G., Bolte, M. & Schneider, C.M. (2005) Self-trapping of magnetic oscillation modes in Landau flux-closure structures. *Phys. Rev. Lett.* **95**, 207201/1–4.

Krasyuk, A., Wegelin, F., Nepijko, S.A., Elmers, H.J., Schönhense, G., Mönch, I., Vinzelberg, H. & Schneider, C.M. (2009) Dynamic of 180° Néel walls in two-dimensional Permalloy particles observed via picosecond time-resolved photoemission electron microscopy. *Ukr. J. Phys.* **54**, 170–175.

Nepijko, S.A., Klais, M., Oelsner, A., *et al.* (2002a) New applications of the magnetic X-ray circular dichroism method for surface magnetism investigations in a photoemission electron microscope. *Appl. Phys.* A **74**, 295–298.

Nepijko, S.A., Klais, M., Schönhense, G., *et al.* (2003) Micromagnetism of two-dimensional Permalloy particles with different aspect ratio. *Appl. Phys.* A **76**, 809–815.

Nepijko, S.A., Sedov, N.N. & Schönhense, G. (2000) Measurement of magnetic fields and domain structures using a photoemission electron microscope. *Advances in Imaging and Electron Physics*, vol. **113**, (ed. by P.W. Hawkes), pp. 205–248. Academic Press, San Diego–San Francisco–New York–Boston–London–Sydney–Tokyo.

Nepijko, S.A., Sedov, N.N., Schönhense, G., Muschiol, U., Schneider, C.M., Zennaro, S. & Zema, N. (2002b) Resolution of an emission electron microscope in the presence of magnetic fields on the object. *Ann. Phys.* **11**, 461–471.

Oelsner, A., Krasyuk, A., Neeb, D., Nepijko, S.A., Kuksov, A., Schneider, C.M. & Schönhense, G. (2004) Magnetization changes visualized using photoemission electron microscopy. *J. Electr. Spectr. Rel. Phenom.* **137–140**, 751–756.

Oelsner, A., Schmidt, O., Schicketanz, M., Klais, M.J., Schönhense, G., Mergel, V., Jagutzki, O. & Schmidt-Böcking, H. (2001) Microspectroscopy and imaging using a delay line detector in time-of-flight photoemission microscopy. *Rev. Sci. Instrum.* **72**, 3968–3974.

Raabe, J., Quitmann, C., Back, C.H., Nolting, F., Johnson, S. & Buehler, C. (2005) Quantitative analysis of magnetic excitations in Landau flux-closure structures using synchrotron-radiation microscopy. *Phys. Rev. Lett.* **94**, 217204/1–4.

Schneider, C.M. & Schönhense, G. (2002) Investigating surface magnetism by means of photoexcitation electron emission microscopy. *Rep. Progr. Phys.* **65**, R1785–R1839.

Stöhr, J., Wu, Y., Samant, M.G., Hermsmeier, B., Harp, G.R., Koranda, S., Dunham, D. & Tonner, B.P. (1993) Element-specific magnetic microscopy with circularly polarized x-ray. *Science* **259**, 658–661.

Vogel, J., Kuch, W., Bonfim, M., *et al.* (2003) Time-resolved magnetic domain imaging by x-ray photoemission electron microscopy. *Appl. Phys. Lett.* **82**, 2299–2301.